Guidelines for Predicting Lesion Size at Common Endocardial Locations During Radio-Frequency Ablation

Supan Tungjitkusolmun, *Member, IEEE*, Vicken R. Vorperian, Naresh Bhavaraju, *Student Member, IEEE*, Hong Cao, *Student Member, IEEE*, Jang-Zern Tsai, *Student Member, IEEE*, and John G. Webster*, *Fellow, IEEE*

***Abstract*—We used the finite element method to study the effect of radio-frequency (RF) catheter ablation on tissue heating and lesion formation at different intracardiac sites exposed to different regional blood velocities. We examined the effect of application of RF current in temperature- and power-controlled mode above and beneath the mitral valve annulus where the regional blood velocities are high and low respectively. We found that for temperature-controlled ablation, more power was delivered to maintain the preset tip temperature at sites of high local blood velocity than at sites of low local blood velocity. This induced more tissue heating and larger lesion volumes than ablations at low velocity regions. In contrast, for power-controlled ablation, tissue heating was less at sites of high compared with low local blood velocity for the same RF power setting. This resulted in smaller lesion volumes at sites of low local velocity.**

Our numerical analyzes showed that during temperature-controlled ablation at 60 °C, the lesion volumes at sites above and underneath the mitral valve were comparable when the duration of RF current application was 10 s. When the duration of RF application was extended to 60 s and 120 s, lesion volumes were 33.3% and 49.4% larger above the mitral valve than underneath the mitral valve. Also, with temperature-controlled ablation, tip temperature settings of 70 °C or greater were associated with a risk of tissue overheating during long ablations at high local blood velocity sites. In power-controlled ablation (20 W), the lesion volume formed underneath the mitral valve was 165.7% larger than the lesion volume above the mitral valve after 10 s of ablation. We summarized the guidelines for energy application at low and high flow regions.

***Index Terms*—Cardiac ablation, catheter ablation, finite element, power-controlled, radio-frequency ablation, temperature-controlled.**

I. Introduction

RADIO-FREQUENCY (RF) catheter ablation technique is the accepted mode of treatment of abnormally rapid heart rates associated with the Wolff–Parkinson–White syndrome (WPW) and other conditions. The efficacy of the RF ablation procedure for the treatment of WPW is very high, and the incidence of complications low [1]. In a healthy human heart, the ventricles are electrically insulated from the atria, except at the atrioventricular (AV) node through which the excitation signal conducts from the atria to the ventricles. When, in addition to the AV node, accessory conduction pathways are present between the atria and the ventricles, the excitation signal may loop between the atria and ventricles via these pathways and the AV node causing rapid heart rates. Application of RF energy to ablate the accessory pathways can restore the heart to a normal condition.

During RF ablation, RF current is deposited from the electrode tip into the tissue. The extent of tissue heating and the volume of myocardial lesion formation depend on multiple variables. Some of the important factors are the electrical and thermal properties of the ablation catheter, cardiac tissue, and blood; the amount and duration of RF energy application; the size of the ablation electrode; the contact of the electrode with the tissue; and the amount of convection heat loss due to the flowing blood in the cardiac chamber [2]. Generally there are two control mechanisms for RF ablation—temperature-controlled, and power-controlled. For both modes, we set the power output and the ablation duration. For temperature-controlled mode we additionally set an electrode tip temperature, the RF generator will then monitor the temperature via a thermistor or a thermocouple mounted at the electrode tip. The control algorithm in the RF generator will try to maintain the tip temperature for the duration of ablation by varying the amount of current delivered to the electrode tip. For power-controlled mode, the generator will deliver the preset maximum power to the ablation electrode.

Fig. 1 shows that the blood velocity is higher at the left atrial surface of the mitral annulus over the leaflet than underneath the valve leaflet and is highest in the aortic outflow tract. RF ablation with same power setting at these three positions results in different tissue heating or lesion volume. Also, RF ablation with the same tip temperature setting at these three positions results in different tissue heating effect. *In vitro* studies have demonstrated that the steady state temperature recorded at the ablation electrode-tissue interface correlates with lesion size [3]. It has also been demonstrated that setting the tip temperature may better predict the formation of an effective RF lesion in the clinical setting [4]; however, no *in vivo* correlation between electrode tip temperature and lesion size has been demonstrated during ablation at different intracardiac sites.

Manuscript received November 17, 1999; revised October 2, 2000. This work was supported by the National Institutes of Health (NIH) under Grant HL56143. *Asterisk indicates corresponding author.*

S. Tungjitkusolmun is with the Department of Electronics Engineering, King Mongkut's Institute of Technology Ladkrabang, Ladkrabang, Bangkok, 10520 Thailand.

V. R. Vorperian is with the Department of Medicine, University of Wisconsin, Madison, WI 53792 USA.

N. Bhavaraju is with the Biomedical Engineering Program, University of Texas at Austin, Austin, TX 78712 USA.

H. Cao and J.-Z. Tsai are with the Department of Electrical and Computer Engineering, University of Wisconsin, Madison, WI 53706 USA.

*J. G. Webster is with the Department of Biomedical Engineering, University of Wisconsin, 1415 Engineering Dr., Madison, WI 53706 USA (e-mail: webster@engr.wisc.edu).

Publisher Item Identifier S 0018-9294(01)00571-7.

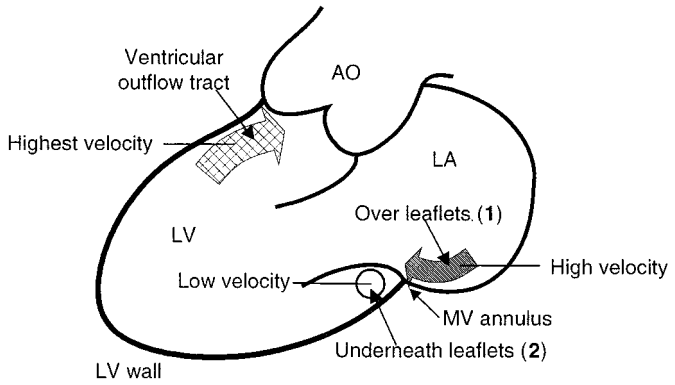

Fig. 1. Blood velocity is higher at the atrial surface of the annulus over the leaflet (position 1, stripes) than underneath the valve leaflet (location 2, circle) and is highest in the outflow tract (cross hatch). RF ablation with same power setting at these three positions results in different tissue heating or lesion volume. Also, RF ablation with the same tip temperature setting at these three positions results in different tissue heating effect.

We utilized the finite element (FE) method to better define target-dependent differences in the effectiveness of tissue heating during RF ablations by taking into account local tissue properties, the local convective film coefficient (cooling effect of local blood velocity) and catheter specification on tissue temperature profile. We have utilized FE analyses for studies of new electrode designs [5], [6]. The purpose of this paper is to discuss some of the variables—contact, ablation site, convective cooling, ablation duration, and mode of ablation (temperature- or power-controlled)—that affect lesion formation. This will provide tip temperature or power setting guidelines that would enable the operator to control the lesion volume at a given target ablation site when ablation is performed with conventional catheters.

II. Finite Element Model

A. The Bioheat Equation

The mechanism by which RF current induces tissue injury is the conversion of electric energy into heat. The circuit consists of the RF generator, the connecting wire to the electrode, the myocardium (and other tissues in the torso), a surface dispersive electrode, and the connecting wires to the generator that will close the electric circuit. Joule heating arises when energy dissipated by an electric current flowing through a conductor is converted into thermal energy. The bioheat equation (1) governs heating during cardiac ablation

$$\rho c \frac{\partial T}{\partial t} = \nabla \cdot k \nabla T + \boldsymbol{J} \cdot \boldsymbol{E} - Q_h \tag{1}$$

where

- T temperature distribution (°C);
- ρ density (g/mm^3);
- c specific heat [J/(g·K)];
- k thermal conductivity [W/(mm·K)];
- $\boldsymbol{J}$ current density (A/mm^2);
- $\boldsymbol{E}$ electric field intensity (V/mm);
- Q_h heat loss due to blood perfusion in the myocardial wall. Q_h is neglected since it is small [3].

We used the material properties from the literature [7], [8]. We used a change of 2%/°C of myocardial conductivity, and the temperature-dependent thermal conductivity and the specific heat of the myocardium [9], [10]. We modeled the electrode as described by Edwards and Stern, 1997 [11]. Myocardial injury occurs once the temperature reaches approximately 50 °C [12]. An optimal RF ablation procedure should be able to heat the desired tissue above 50 °C without heating the tissue above 100 °C when popping occurs.

For all of the simulations performed in this paper, the ablation electrode was of standard size used in clinical practice (4 mm long, and 2.6-mm diameter). A temperature sensing thermistor was embedded at the electrode tip and the catheter tip was pushed into the myocardium for variable distances. The blood pool extended 40 mm beyond the myocardium. We set the temperature of the blood on the boundary of the model to 37 °C due to the blood flow in the cardiac chamber. Using the Dirichlet boundary conditions, we assumed that the voltages on the outer surfaces of the model were 0 V. To simulate constant power-controlled ablation or temperature-controlled ablation, we adjusted the voltage applied to the electrode after each time step on a trial and error basis. We simulated ablation for 120 s, with time steps ranging from 0.1 to 1 s for the first 5 s of ablation and 1 s thereafter.

B. Convection Film Coefficients and Local Blood Velocity Measurement

We can calculate the heat fluxes at the blood-catheter, and the blood-tissue interfaces by

$$k \frac{\partial T}{\partial \boldsymbol{n}} = h_b (T - T_{bl}) \tag{2}$$

where

- h_b convective film coefficient due to the blood flow [W/(m^2·K)];
- T_{bl} blood temperature (constant at 37 °C);
- $\boldsymbol{n}$ unit vector normal to the myocardial or the electrode surface.

The cooling effect of flowing blood depends on the locations in the cardiac chamber. The values of the h_b at the blood-myocardium and at the blood-electrode interfaces are different. We used h_b for the blood-myocardium interfaces from Bhavaraju *et al.* [13] who measured the heat transfer coefficient in a physical model of a swine heart under a pulsatile flow condition (0.9 to 6.8 L/min). The ablation electrode is inside the flowing blood in the cardiac chamber. h_b at the blood-electrode interface varies, depending on the position of the electrode in the cardiac chamber. Since the shape of the electrode is cylindrical, we can make analytical estimates for the values of h_b. The tip of the electrode is spherical but it is embedded into the tissue. It is assumed that the electrode can be modeled as a cylinder in a cross flow. The heat-transfer coefficient at the blood-electrode interface (h_{be})

$$h_{be} = \frac{\mathrm{Nu}k}{d} \tag{3}$$

where the Nusselt number (Nu) is given by

$$\mathrm{Nu} = 0.683 \mathrm{Re}^{0.466} \mathrm{Pr}^{1/3} \tag{4}$$

the Prandtl number (Pr) is 25, and the Reynolds number (Re) is

$$\mathrm{Re} = \frac{\rho v d}{\mu} \tag{5}$$

TABLE I
IN THE FE MODELS, THE BLOOD VELOCITIES ($N = 5$) AND THE CONVECTIVE FILM COEFFICIENTS ARE HIGHER IN POSITION 1 (ABOVE THE MITRAL VALVE) THAN IN POSITION 2 (UNDERNEATH THE MITRAL VALVE). *BLOOD VELOCITY AT POSITION 2 WAS ESTIMATED AS 10% OF THE BLOOD VELOCITY AT POSITION 1

Location	Blood velocity (cm/s)	h_b at blood–myocardium interface [(W/(m^2·K)]	h_{be} at blood–electrode interface [W/(m^2·K)]
Position 1	24.4 ± 6.8	1417	6090
Position 2	2.4*	44	2081

where
- d diameter of the electrode (2.6 mm);
- v blood velocity;
- μ viscosity of blood [(0.0021 kg/(m·s)] [14].

We determined the blood velocities in the cardiac chamber by Doppler [15]. We used an ultrasound transducer to measure the blood velocities above the mitral valve leaflets in five human subjects ($N = 5$). Although the blood velocities varied during a cardiac cycle, we used the average velocities to calculate the heat transfer coefficients in order to simplify our FE models. The blood velocities in the recess underneath the mitral valve leaflets could not be measured due to noise interferences from the moving heart and the smaller areas. Thus, we estimated that the blood velocities in the deeper recesses underneath the mitral valve leaflets, where the ablation electrode tip would be lodged, were approximately 10% of those above the mitral valve leaflets. The flow patterns in the cardiac chamber are highly turbulent, hence the estimates obtained could be lower than the actual heat transfer coefficients. Table I summarizes the convective film coefficients above the mitral valve and underneath the mitral valve leaflets for the blood-myocardium and blood-electrode interfaces.

C. Software

We used PATRAN version 7.0 (The MacNeal–Schwendler Co., Los Angeles) as a preprocessor for FE Models in this study. PATRAN allows users to create the geometric model, assign material properties to the appropriate regions, as well as the boundary conditions and loads. We can also mesh the models with PATRAN and then instruct it to generate an input file for the ABAQUS/Standard solver. We used ABAQUS version 5.8 (Hibbitt, Karlsson & Sorensen, Inc., Pawtucket, RI) to solve the thermal-electric FE analyzes. We ran all numerical problems on our HP-C180 workstation (with 1152 MB of RAM and about 34 GB of total disk space. A built-in module in ABAQUS, ABAQUS/POST allowed us to perform postprocessing of our numerical results.

III. ABLATIONS OF ACCESSORY PATHWAYS

Electrophysiologists can ablate the accessory pathways using different approaches. Generally, when ablating an accessory pathway from the ventricular aspect of the mitral valve annulus there is lower blood flow at the ablation site. Also, the recessed anatomy of region permits good contact between the ablation electrode and the cardiac muscle. When the ablating catheter is further advanced, via a retrograde aortic approach, to reach the atrial aspect of the mitral valve annulus, contact is more difficult to establish because an anatomical recess, which would permit for catheter tip "foothold," does not exist. Also, there is higher blood flow at such an ablation site. Fig. 2(a) and (b) illustrates modeled contacts between the catheter and the myocardium for the two cases mentioned above for the retrograde aortic approach. The two crucial parameters—contact, and the cooling effect from flowing blood—are different in the two cases. Table II lists the characteristics of different ablation sites.

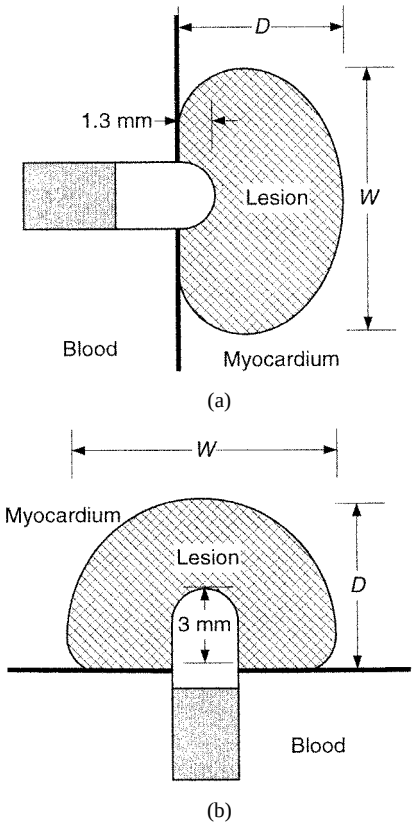

Fig. 2. (a) Position 1. For ablation above the mitral valve annulus, the tip of the electrode is embedded 1.3 mm into the myocardium. (b) Position 2. For ablation underneath the mitral valve annulus, the ablation electrode is embedded 3 mm into the myocardium. D is the lesion depth (measured from the myocardial surface), and W is the lesion width.

TABLE II
ABOVE THE MITRAL VALVE, THE BLOOD FLOW IS HIGHER, AND THE CONTACT AREA (1.3 mm) IS SMALLER THAN WHEN ABLATING UNDERNEATH THE MITRAL VALVE (3 mm)

Position	Contact	Blood flow
1. Above the mitral valve	1.3 mm embedded	High
2. Underneath the mitral valve	3.0 mm embedded	Low

We simulated the numerical models for up to 120 s ablation, or once the maximum temperature reached 100 °C (whichever came first). We created two FE models to represent RF ablation for the atrial and the ventricular approaches for left-sided accessory pathways.

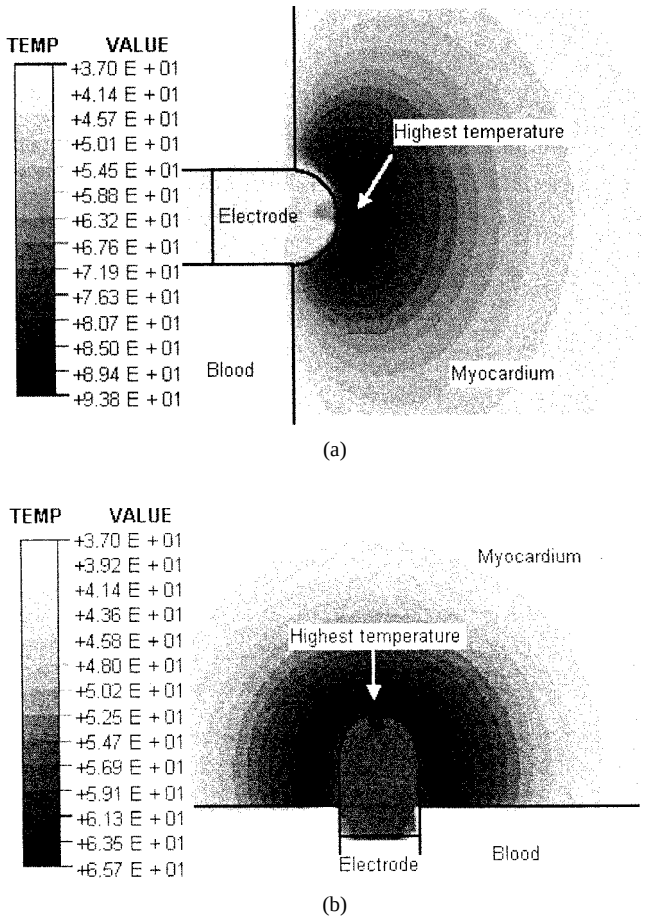

Fig. 3. Temperature distribution in the temperature-controlled ablation ($T_{\text{tip}} = 60$ °C), after 60 s. (a) Position 1. (b) Position 2.

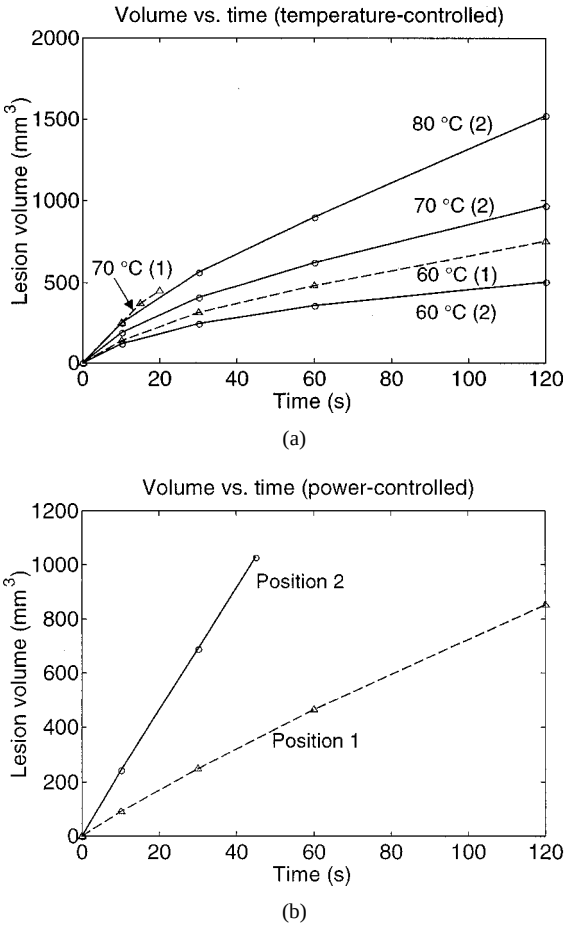

Fig. 4. Lesion dimensions versus time. (a) Temperature-controlled ablation. (b) Constant power-controlled ablation (20 W). The dashed line represents ablation at position 1 (above MV valve), and the solid line represents ablation at position 2 (underneath MV valve).

A. Position 1 (Ablation Over the Mitral Valve Annulus)

The electrode tip is embedded 1.3 mm into the myocardial wall [Fig. 2(a)]. The cooling effect from the flowing blood is high at this location. We used h_b for the blood-myocardium and blood-electrode interfaces listed in Table I. We simulated ablations for both the temperature-controlled (preset tip temperature of 60 °C and 70 °C) and power-controlled (20 W) ablation. The axisymmetric FE model in this case contained 17 214 nonuniformly meshed elements.

B. Position 2 (Ablation Underneath the Mitral Valve Leaflets)

The electrode tip is embedded 3 mm into the myocardium [Fig. 2(b)]. The cooling effect from the flowing blood in this area is lower than that at position 1. Thus, we assign lower convective film coefficients at the myocardium-blood interface, and the electrode-blood interface in this case (Table I). We performed simulations for both the temperature-controlled (60 °C, 70 °C, and 80 °C) and power-controlled (20 W) ablation. The axisymmetric FE model in this case contained 18 435 nonuniformly meshed elements.

IV. Results

A. Temperature Distributions

Fig. 3(a) and (b) shows the temperature distributions after 60 s of temperature-controlled ablation (60 °C) at position 1, and 2, respectively. We observe that the temperature distribution at position 1 is less uniform than that at position 2 (for position 1, the hottest areas are located at the regions to the right of the tip, while the hottest areas for position 2 surround the electrode). This was due to effect of flowing blood in the cardiac chamber. There was a large temperature gradient between the myocardial surface and the region deep into the myocardium. In both cases, the "hot spots" (locations with the highest temperature) were not at the tip of the ablation electrode, but they were a fraction of a millimeter away from the electrode tip. Thus, the thermistor located at the tip of the ablation catheter tends to underestimate the maximum myocardial temperature. After 60 s of ablation, the tip temperature stayed at 60 °C but the maximum tissue temperature was over 90 °C at position 1. In contrast, in the low-flow region (position 2), the temperature difference between the electrode tip and the maximum tissue temperature was only 5.7 °C.

B. Lesion Volumes

The shape and size of a lesion was determined from the 50 °C contour of the temperature distribution after RF applied duration. Fig. 4(a) and (b) shows the results for the lesion volumes versus time throughout 120 s of ablation. For a preset tip temperature of 60 °C, the lesion volume at position 1 was consistently higher than that at position 2 throughout 120 s of abla-

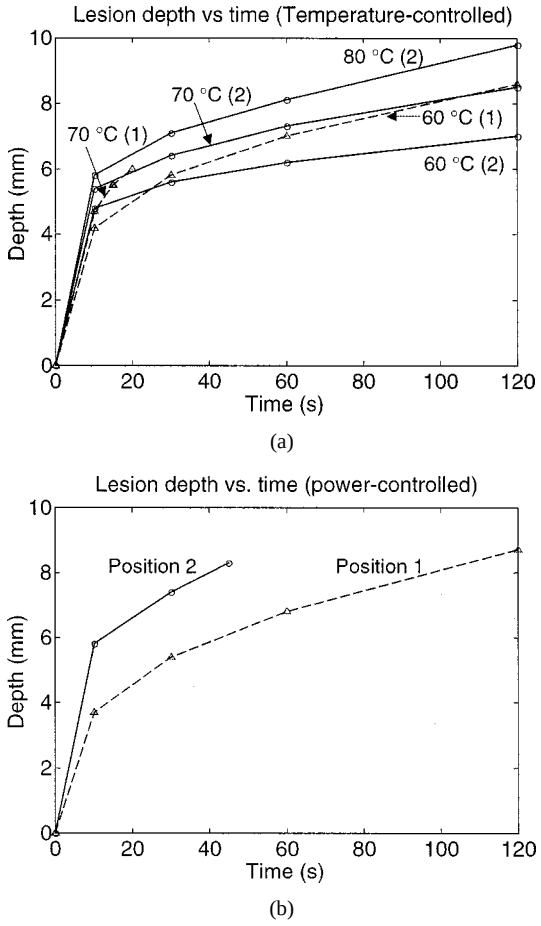

Fig. 5. Lesion depth versus time. (a) Temperature-controlled ablation. (b) Power-controlled ablation.

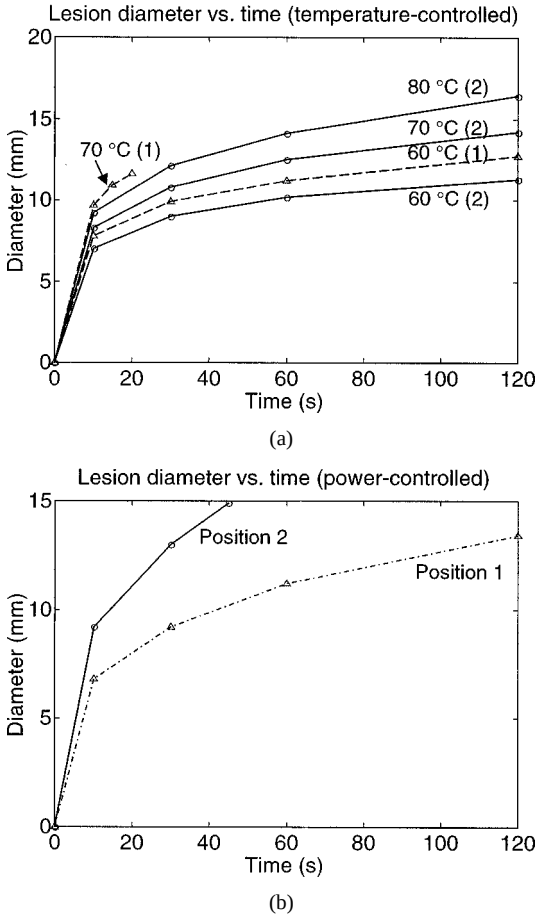

Fig. 6. Lesion diameter versus time. (a) Temperature-controlled ablation. (b) Power-controlled ablation.

tion (139.1 mm^3 versus 118.0 mm^3 after 10 s, and 753.0 mm^3 versus 504.1 mm^3 after 120 s). The total energy delivered after 10 s was 282 J at position 1, and 101 J at position 2. The lesion volumes were higher when we increased the preset tip temperature. Note that for ablation at position 1 with a preset tip temperature of 70 °C, we stopped the simulation after 20 s because the maximum tissue temperature reached 100 °C. In other cases, the lesion volumes continued to grow over time even after 60 s.

In power-controlled ablation, the lesion volume at position 2 was larger than that at position 1. We terminated the simulation at position 2 after 45 s, when the maximum myocardial temperature reached 100 °C. There was less heat loss due to the cooling effect at position 2, thus, a power of 20 W was sufficient to heat the myocardium at position 2 than at position 1. Since there was higher cooling effect from the blood at position 1, the lesion volume was smaller, and it continued to grow over time. The maximum tissue temperature at position 1 did not exceed 100 °C after 120 s.

C. Lesion Depths

Fig. 5(a) and (b) shows that the general trend of the lesion depths over time follows that of the lesion volumes. For the same set tip temperature, the lesion depth at position 2 was higher than that at position 1 during the first 20 s of ablation, and the lesion depth at position 1 was deeper afterwards. In temperature-controlled ablation, the maximum lesion depth at position 1 (60 °C tip temperature) was 8.6 mm after 120 s, and the maximum depths at position 2 were 7.0 mm (60 °C) and 9.8 mm (80 °C) after 120 s. In power-controlled ablation, the maximum depths at positions 1 and 2 were 8.7 mm (after 120 s) and 8.3 mm (after 45 s), respectively. The lesion depths in these cases were measured from the myocardial surface. Thus, a 5-mm depth for ablations at position 2 means that the lesion extended 2 mm beyond the tip of the electrode (the electrode tip was embedded 3 mm into the myocardium).

D. Lesion Diameters

Fig. 6(a) and (b) shows the maximum lesion diameters over time. When the set tip temperature was 60 °C, the lesion diameter at position 1 was slightly larger than the lesion diameters at position 2 (12.7 mm versus 11.3 mm after 120 s). In power-controlled ablation, the maximum lesion diameter at position 1 was 13.4 mm (120 s) and the maximum lesion depth at position 2 was 14.9 mm (45 s).

E. Maximum Temperatures and Their Locations

For 60 °C preset tip temperature, the maximum temperature reached in the myocardium was much higher at position 1 than that at position 2 (94.6 °C versus 66.3 °C) after 120 s. Fig. 7(a) and (b) shows the maximum temperatures reached in the myocardium over time. As mentioned in Section IV-B,

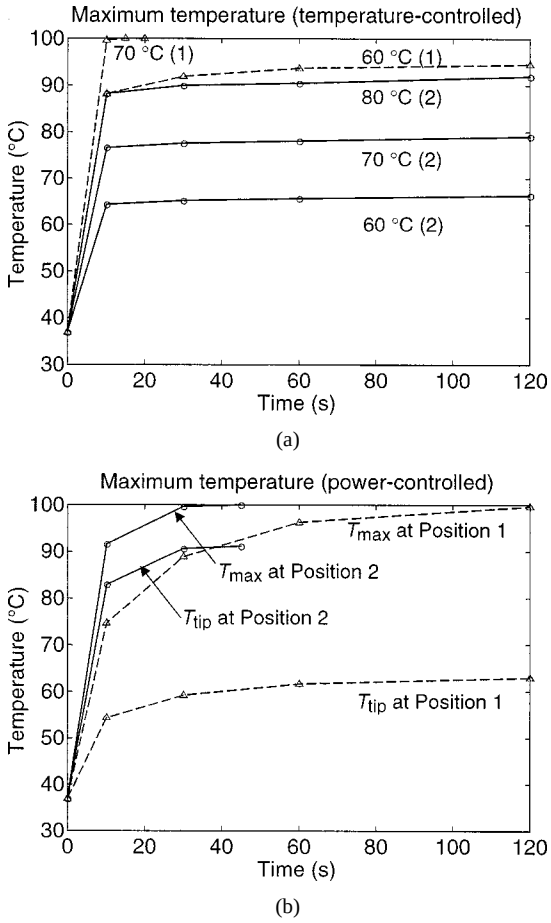

Fig. 7. Maxium temperature versus time. (a) Temperature-controlled ablation. (b) Power-controlled ablation.

the maximum temperature at position 2 reached 100 °C after 45 s in the power-controlled ablation. The location for the maximum myocardial temperature moved from 0.6 mm from the tip after 10 s to 0.8 mm after 120 s for temperature-controlled and power-controlled ablation at position 1, and it moved from 0.4 to 0.6 mm for temperature-controlled ablation at position 2. For power-controlled ablation at position 2, the maximum myocardial temperature was at 0.2 mm after 10 s, and at 0.3 mm after 50 s. The tip temperature at position 1 reached 54.4 °C at 10 s, and 62.9 °C at 120 s, 20 W ablation. The tip temperatures at position 2 were 82.9 °C at 10 s, and 91.1 °C at 45 s (when the maximal myocardial temperature exceeded 100 °C).

V. Discussion

The results from our FE analyses suggest that when RF ablations are performed in regions with higher blood flow, the temperature recorded at the catheter tip underestimates the maximum temperature within the tissue. In such a scenario, if a temperature of 80 °C is achieved at the catheter tip, the maximum tissue temperature may be well over 100 °C. Relying on the tip-temperature alone might lead to overheating of cardiac tissue and to popping.

Differences in lesion volumes in different ablation sites are related to the differences in convective cooling of the electrode tip in the heart and the electrode-tissue contact. After 10 s of ablation in 60 °C temperature-controlled ablation, the lesion volumes at positions 1 and 2 were comparable. After 120 s, the lesion dimensions are clearly larger at position 1. For 70 °C ablation at position 1, it was not possible to complete a full cycle of RF ablation (120 s) because the maximum myocardial temperature reached 100 °C after 30 s. Different RF generators have different controlling algorithms that account for the thermal inertia of the system. Thus, in real settings, the longer duration of ablation might be possible. In contrast to temperature-controlled ablation, the power is preset in power-controlled ablation, and the reached tip temperature will reflect the quality of electrode-tissue contact and convective cooling caused by intracavitary blood flow.

A. Summary of Results

In this study we used the FE method to examine clinically relevant RF temperature, power and duration settings. Based on our findings, we summarize the guidelines for ablations at different sites.

1) For temperature-controlled ablation in areas with high convective cooling, e.g., ablation of slow pathways in AV node reentrant tachycardia, ablation of accessory pathways using the atrial approach, we recommend a lower preset tip temperature for the atrial approach in order to avoid overheating of the myocardium. In areas with low convective cooling, such as the apex or ventricular aneurysms, the catheter tip temperature gives a closer estimate of the maximum myocardial temperature.
2) There is a positive correlation between lesion volumes and the preset tip temperatures for ablations in low flow regions.
3) For power-controlled ablation, we recommend higher preset power for ablation in high flow regions (e.g., position 1), and lower preset power for ablation in low flow regions (e.g., position 2). There is a risk of overheating the myocardium in the low flow region for long duration ablation. Our finding correlates with a previous clinical study [16].
4) The maximum tissue temperature continues to increase over time. Our FE models indicated that the maximum tissue temperature rose rapidly during the first 10 s of RF ablation. It will continue to rise though at a slower rate in extended treatment duration. This is most evident in the case of power-controlled ablation at position 1 (high flow). It was generally believed that the myocardium temperature reached steady state after 10 s [4].
5) The lesion volumes grow quickly during the first 10 s of ablation and they continue to grow over long duration ablation. By setting a low preset tip temperature ($<60°C$), and ablating the myocardium for a longer duration, we can create larger lesion volumes.

Acknowledgment

The authors wish to thank Dr. P. S. Rahko of the Department of Medicine, University of Wisconsin-Madison, for his help with Doppler measurements of blood velocities.

REFERENCES

[1] S. Willem, X. Chen, H. Kottkam, G. Hindricks, W. Haverkamp, B. Rotman, M. Shenasa, G. Breithardt, and M. Borggrefe, "Temperature-controlled radiofrequency catheter ablation of manifest accessory pathways," *Eur. Heart J.*, vol. 17, pp. 445–52, 1996.

[2] S. K. S. Huang and D. J. Wilber, Eds., *Radiofrequency Catheter Ablation of Cardiac Arrhythmias: Basic Concepts and Clinical Applications*, 2nd ed. Armonk, New York: Futura, 2000.

[3] D. E. Haines and D. D. Watson, "Tissue heating during radiofrequency catheter ablation: A thermodynamic model and observation in isolated perfused and superfused canine right ventricular free wall," *PACE*, vol. 12, pp. 962–976, 1989.

[4] J. J. Langberg, H. Calkins, R. El-Atassi, M. Borganelli, A. Leon, S. J. Kalbfleisch, and F. Morady, "Temperature monitoring during radiofrequency catheter ablation of accessory pathways," *Circulation*, vol. 86, pp. 1469–1474, 1992.

[5] E. J. Woo, S. Tungjitkusolmun, H. Cao, J.-Z. Tsai, J. G. Webster, and V. R. Vorperian, "A new catheter design using needle electrode for subendocardial RF ablation of ventricular muscles: finite element analysis and in vitro experiments," *IEEE Trans. Biomed. Eng.*, vol. 47, pp. 23–31, Jan. 2000.

[6] S. Tungjitkusolmun, E. J. Woo, H. Cao, J.-Z. Tsai, V. R. Vorperian, and J. G. Webster, "Finite element analyses of uniform current density electrodes for radio-frequency cardiac ablation," *IEEE Trans. Biomed. Eng.*, vol. 47, pp. 32–40, Jan. 2000.

[7] D. Panescu, J. G. Whayne, D. Fleischman, M. S. Mirotznik, D. K. Swanson, and J. G. Webster, "Three-dimensional finite element analysis of current density and temperature distributions during radio-frequency ablation," *IEEE. Trans. Biomed. Eng.*, vol. 42, pp. 870–890, 1995.

[8] S. Tungjitkusolmun, E. J. Woo, H. Cao, J. Tsai, V. R. Vorperian, and J. G. Webster, "Thermal-electrical finite element modeling for radio-frequency cardiac ablation: Effects of changes in myocardial properties," *Med. Biol. Eng. Comput.*, vol. 38, pp. 562–568, 2000.

[9] K. R. Foster and H. P. Schwan, "Dielectric properties of tissues and biological materials: a critical review," *CRC Crit. Rev. Biomed. Eng.*, vol. 17, pp. 25–104, 1989.

[10] N. C. Bhavaraju and J. W. Valvano, "Thermophysical properties of swine myocardium," *Int. J. Thermophys.*, vol. 20, pp. 665–676, 1999.

[11] S. D. Edwards and R. A. Stern, "Electrode and associated systems using thermally insulated temperature sensing elements," U. S. Patent no. 5 688 266, 1997.

[12] S. Nath, C. Lynch III, J. G. Whayne, and D. E. Haines, "Cellular electrophysiological effects of hyperthermia on isolated Guinea pig papillary muscle: Implications for catheter ablation," *Circulation*, pt. 1, vol. 88, pp. 1826–1831, 1993.

[13] N. C. Bhavaraju, "Heat transfer modeling during radiofrequency cardiac ablation in swine myocardium," Ph.D. Dissertation, Univ. Texas, Austin, Mar. 2000.

[14] F. P. Incropera and D. P. DeWitt, *Fundamentals of Heat and Mass Transfer*, 3rd ed. New York: Wiley, 1990.

[15] A. B. Houston and I. A. Simpson, Eds., *Cardiac Doppler Ultrasound: A Clinical Perspective*. Boston: Wright, 1988.

[16] S. A. Strickberger, J. Hummel, M. Gallagher, C. Hasse, K. C. Man, B. Williamson, V. R. Vorperian, S. J. Kalbfleisch, F. Morady, and J. J. Langberg, "Effect of accessory pathway location on the efficiency of heating during radiofrequency catheter ablation," *Amer. Heart. J.*, vol. 129, pp. 54–8, 1995.

Supan Tungjitkusolmun (S'96–M'00) was born in Bangkok, Thailand, on December 5, 1972. He received the B.S.E.E. degree from the University of Pennsylvania, Philadelphia, PA, in 1995, and the M.S.E.E. and Ph.D. degrees from the University of Wisconsin, Madison, WI, in 1996, and 2000, respectively.

He is on the faculty of the Department of Electronics Engineering, King Mongkut's Institute of Technology Ladkrabang (KMITL), Bangkok, Thailand. His research interests include finite element modeling, radio-frequency cardiac ablation, and hepatic ablation. He is contributing author to J. G. Webster (Ed.), *Design of Pulse Oximeters* (Bristol, UK: IOP Publishing, 1997).

Dr. Tungjitkusolmun was a recipient of the Royal Thai Government Scholarship from 1990 to 2000. He is a member of Tau Beta Pi, Eta Kappa Nu, and Pi Mu Epsilon.

Vicken R. Vorperian received the B.S. degree in biology and chemistry in 1979 and the M.D. degree in 1985, both from the American University of Beirut, Lebanon. He then completed the following postgraduate medical clinical training programs: internship and residency in the specialty of internal medicine from 1985–1988 at the Sinai Hospital of Baltimore, Baltimore, MD; fellowship in the subspecialty of cardiology from 1988–1990 at the Brooklyn Hospital, Brooklyn, NY; fellowship in cardiac arrhythmias and electrophysiology at the Vanderbilt University, Nashville, TN; fellowship in cardiac pacing and catheter ablation at the University of Michigan, Ann Arbor, MI. He received his Board Certification in the specialty of Internal Medicine in 1988, in Cardiology in 1991, and in Clinical Cardiac Electrophysiology in 1994 from the American Board of Internal Medicine.

He is an Associate Scientist in the cardiac RF ablation project in the Department of Biomedical Engineering. He holds the title of Clinical Associate Professor of Medicine in the section of Cardiology, Department of Medicine, University of Wisconsin-Madison and is an Attending Electrophysiologist in the Cardiac Electrophysiology Laboratory at the University of Wisconsin Hospital-Madison. He is also a Member of the Arrhythmia Consultants of Milwaukee S.C., a private practice group in cardiac arrhythmias and clinical cardiac electrophysiology. His research interests in cardiac electrophysiology include the design of experimental setups to address questions about different aspects of RF catheter ablation of arrhythmias in the clinical setting. His research interests also include the clinical and basic electrophysiologic properties of newer and developmental antiarrhythmic agents.

Naresh C. Bhavaraju (S'97) received his B.E in electrical engineering from Andhra University, Visakhapatnam, India in 1993, M.Tech. in control engineering and instrumentation from Indian Institute of Technology, Delhi, India in 1994 and Ph.D. in biomedical engineering from The University of Texas at Austin, TX in 2000.

He is currently a Member of the technical staff of Flint Hills Scientific, L.L.C., Lawrence, KS. His research interests include hardware and software design for improving therapeutic techniques, safety issues of bioinstrumentation, signal processing, and finite element modeling.

Dr. Bhavaraju is also a Member Tau Beta Pi and AAMI.

Hong Cao (S'97) received the B.S.E.E. and M.S.E.E. degrees from Nanjing University, Nanjing, China, in 1992 and 1995, respectively. He is currently a Ph.D. candidate in the Department of Electrical and Computer Engineering at the University of Wisconsin-Madison.

His research interests include temperature measurement inside myocardium during RF catheter ablation and optimization of catheter design.

Jang-Zern Tsai (S'97) was born in Chia-Yi, Taiwan, in 1961. He received the B.S.E.E. degree from National Central University, Chung-Li, Taiwan, in 1984, and the M.S.E.E. degree from National Tsing Hua University, Hsinchu, Taiwan, in 1986. In 1986, he joined the Electronics Research and Service Organization (ERSO) of the Industrial Technology Research Institute (ITRI) as an integrated circuit applications engineer. In 1990, he joined the Computer and Communication Research Laboratories (CCL) of ITRI and worked as a Hardware Engineer on digital recording technology. In 1994, he joined the Accton Technology Corporation as a Computer Network Software Engineer. All companies are located in Taiwan. He is currently a Ph.D. student in the Department of Electrical and Computer Engineering, University of Wisconsin at Madison, WI, doing research on radio-frequency cardiac ablation. His current research interest is myocardial resistivity measurement.

John G. Webster (M'59–SM'69–F'86–LF'97) received the B.E.E. degree from Cornell University, Ithaca, NY, in 1953, and the M.S.E.E. and Ph.D. degrees from the University of Rochester, Rochester, NY, in 1965 and 1967, respectively.

He is Professor of Biomedical Engineering at the University of Wisconsin-Madison. In the field of medical instrumentation he teaches undergraduate and graduate courses, and does research on RF cardiac ablation.

He is author of *Transducers and Sensors*, *An IEEE/EAB Individual Learning Program* (Piscataway, NJ: IEEE, 1989). He is coauthor, with B. Jacobson, of *Medicine and Clinical Engineering* (Englewood Cliffs, NJ: Prentice-Hall, 1977), with R. Pallás-Areny, of *Sensors and Signal Conditioning*, 2nd ed. (New York: Wiley, 2001) and with R. Pallá-Areny, of *Analog Signal Processing* (New York: Wiley, 1999). He is Editor of *Encyclopedia of Medical Devices and Instrumentation* (New York: Wiley, 1988), *Tactile Sensors for Robotics and Medicine* (New York: Wiley, 1988), *Electrical Impedance Tomography* (Bristol, UK: Adam Hilger, 1990), *Teaching Design in Electrical Engineering* (Piscataway, NJ: Educational Activities Board, IEEE, 1990), *Prevention of Pressure Sores: Engineering and Clinical Aspects* (Bristol, UK: Adam Hilger, 1991), *Design of Cardiac Pacemakers* (Piscataway, NJ: IEEE Press, 1995), *Design of Pulse Oximeters* (Bristol, UK: IOP Publishing, 1997), *Medical Instrumentation: Application and Design*, Third Edition (New York: Wiley, 1998), *Handbook of Measurement, Instrumentation, and Sensors* (CRC Press, Boca Raton, FL, 1999), *Encyclopedia of Electrical and Electronics Engineering* (New York: Wiley, 1999), *Mechanical Variables Measurement* (CRC Press, Boca Raton, FL, 2000), and *Minimally Invasive Medical Technology* (Bristol, U.K.: IOP, 2001). He is Coeditor, with A. M. Cook, of *Clinical Engineering: Principles and Practices* (Englewood Cliffs, NJ: Prentice-Hall, 1979) and *Therapeutic Medical Devices: Application and Design* (Englewood Cliffs, NJ: Prentice-Hall, 1982), with W. J. Tompkins, of *Design of Microcomputer-Based Medical Instrumentation* (Englewood Cliffs, NJ: Prentice-Hall, 1981) and *Interfacing Sensors to the IBM PC* (Englewood Cliffs, NJ: Prentice Hall, 1988), and with A. M. Cook, W. J. Tompkins, and G. C. Vanderheiden, of *Electronic Devices for Rehabilitation* (London: Chapman & Hall, 1985).

Dr. Webster has been a Member of the IEEE-EMBS Administrative Committee and the NIH Surgery and Bioengineering Study Section. He is a Fellow of the Instrument Society of America, the American Institute of Medical and Biological Engineering, and the Institute of Physics. He is the recipient of the AAMI Foundation Laufman-Greatbatch Prize, the ASEE/Biomedical Engineering Division, Theo C. Pilkington Outstanding Educator Award and the ASEE/Engineering Libraries Division, Best Reference Work Award.